

Original Article

Therapeutic evaluation of monoclonal antibody-maytansinoid conjugate as a model of RON-targeted drug delivery for pancreatic cancer treatment

Hang-Ping Yao^{1,2*}, Liang Feng^{3,4*}, Jian-Wei Zhou⁵, Rui-Wen Zhang⁶, Ming-Hai Wang^{1,2,3,4}

¹State Key Laboratory for Diagnosis and Treatment of Infectious Diseases and ²Collaborative Innovation Center for Diagnosis and Treatment of Infectious Diseases, First Affiliated Hospital of Zhejiang University School of Medicine, Hangzhou, China; ³Cancer Biology Research Center and ⁴Department of Biomedical Sciences, Texas Tech University Health Sciences Center School of Pharmacy, Amarillo, TX 79106, USA; ⁵Department of Molecular Cell Biology and Toxicology, Nanjing Medical University School of Public Health, Nanjing, China; ⁶Department of Pharmaceutical Sciences, Texas Tech University Health Sciences Center School of Pharmacy, Amarillo, TX 79106, USA. *Equal contributors.

Received February 29, 2016; Accepted March 6, 2016; Epub May 1, 2016; Published May 15, 2016

Abstract: Aberrant expression of the RON receptor tyrosine kinase, a member of the MET proto-oncogene family, contributes significantly to pancreatic cancer tumorigenesis and chemoresistance. Here we validate RON as a target for pancreatic cancer therapy using a novel anti-RON antibody Zt/g4-drug maytansinoid conjugates (Zt/g4-DM1) as a model for RON-targeted drug delivery to kill pancreatic cancer cells. In pancreatic cancer cell lines overexpressing RON, Zt/g4-DM1 rapidly induced receptor endocytosis, arrested cell cycle at G2/M phase, reduced cell viability, and subsequently caused massive cell death. These *in vitro* observations help to establish a correlation between the number of the cell surface RON receptors and the efficacy of Zt/g4-DM1 in reduction of cell viability. In mice, Zt/g4-DM1 pharmacokinetics in the linear dose range fitted into a two-compartment model with clearance in 0.21 ml/day/kg and terminal half-life at 6.05 days. These results helped to confirm a concentration-activity relationship for the BxPC-3 and other pancreatic cancer cell xenograft model with a tumoricidal dose at 3.02 mg/kg. Zt/g4-DM1 was effective *in vivo* against various xenograft PDAC growth but efficacy varied with individual cell lines. Combination of Zt/g4-DM1 with gemcitabine had a complete inhibition of xenograft pancreatic cancer growth. We conclude from these studies that increased RON expression in pancreatic cancer cells is a suitable targeting moiety for anti-RON ADC-directed drug delivery and anticancer therapy. Zt/g4-DM1 is highly effective alone or in combination with chemotherapeutics in inhibition of pancreatic cancer xenograft growth in preclinical models. These findings justify the use of humanized Zt/g4-DM1 for targeted pancreatic cancer therapy in the future.

Keywords: Receptor tyrosine kinase, antibody-drug conjugate, pancreatic cancer, pharmacokinetics, xenograft tumor model, therapeutic efficacy, combination therapy

Introduction

Pancreatic ductal adenocarcinoma (PDAC) is one of the most aggressive cancers with poor prognosis and high mortality [1]. Currently, genetic events associated with PDAC pathogenesis, including mutations or deletions of K-RAS, cyclin-dependent kinase inhibitor 2A (CDKN2A), P53, and signal of mothers against decapentaplegic (SMAD) 4, have been characterized [2-4]. Nonetheless, these abnormalities

have not been translated into clinical practice as reliable PDAC biomarkers for detecting early cancer, evaluating chemotherapy response, and predicting patient survival [1-6]. Another clinical challenge is the poor progress in finding effective therapeutics to treat PDAC. Only a few chemotherapeutics, including gemcitabine, oxaliplatin, and epithelial growth factor receptor (EGFR)-specific tyrosine kinase inhibitor erlotinib are currently available for palliative therapy [1-3]. Thus, identification of reliable bio-

markers to predict PDAC patient survival and development of novel and effective biotherapeutics are greatly needed to combat this deadly disease.

The role of the *recepteur d'origine nantaïs* (RON) receptor tyrosine kinase (RTK) in PDAC pathogenesis has been under intensive investigation [7-17]. The objectives are to determine mechanisms of RON in regulating PDAC invasive growth; to find the significance of RON in PDAC malignancy; to value RON expression as a prognostic marker for PDAC survival; and to validate RON as a drug target for PDAC treatment [10-17]. Preclinical studies have revealed that aberrant RON expression contributes to PDAC cell invasiveness and chemoresistance [10, 11, 15]. Immunohistochemical (IHC) staining of primary PDAC samples indicates that RON is detected at low levels in normal pancreatic tissues but increases dramatically in primary and metastatic PDAC samples [10, 11, 16, 18, 19]. However, the range of RON overexpression in primary PDAC samples varies in studies due to the use of different antibodies, criteria, and interpretations of results [10, 11, 16, 18, 19]. By immunohistochemical staining using a highly specific and sensitive anti-RON monoclonal antibody (mAb) Zt/f2, we have found more than 35% of primary PDAC samples showing RON overexpression [18]. Similar results were also observed in other report [16, 19]. These observations indicate that aberrant RON expression is a pathological feature in primary PDACs. However, overexpression of RON has not been established as a prognostic marker for PDAC patient survival [16]. In addition, increased RON expression also is not associated with therapeutic responsiveness in surgically resected pancreatic cancer [16]. Currently, RON-specific therapeutics including tyrosine kinase inhibitors (TKI) and therapeutic monoclonal antibodies (TMA) have been used in preclinical PDAC models and clinical trials to determine their anti-cancer efficacies [14, 19, 20-25]. Accumulated evidences indicate that targeted inhibition of RON has the therapeutic effect on PDAC cell growth, migration and survival [19, 21, 23, 25]. However, studies in mouse PDAC xenograft models has observed that the efficacy of RON-specific TKIs and TMAs alone is relatively low with only partial inhibition of tumor growth [19, 21, 23, 25]. Complete inhibition by a single RON-targeted TKI or TMA has

not been observed [14-25]. Thus, there is an urgent need to develop and improve the efficacy of RON-targeted therapeutics.

The present study is to evaluate the therapeutic efficacy of monoclonal antibody (mAb) Zt/g4-drug maytansinoid conjugates (ADC Zt/g4-DM1) as a model of RON targeted drug delivery for PDAC treatments. Zt/g4-DM1 as novel ADC was developed by us for potential cancer therapy [26]. ADC selectively ablates cancer cells by combining the specificity of a target-specific mAb with the delivery of a highly potent cytotoxic agent [27-30]. For this purpose, we first selected a panel of PDAC cell lines expressing different levels of RON as the model. The effect of Zt/g4-DM1 on RON endocytosis, cell cycle change, and cell death were studied. Second, we analyzed plasma pharmacokinetics (PK) of Zt/g4-DM-1 in both tumor-bearing and -nonbearing mice. A dose-time relationship was established to model the efficacy of Zt/g4-DM1 *in vivo* to obtain a tumoricidal concentration. Third, we validated Zt/g4-DM1 activity in inhibition of PDAC growth in mouse xenograft models. The objective is to determine the Zt/g4-DM1 efficacy and to establish a potential therapeutic strategy. Finally, we discovered an increase in tumor inhibition by combination of Zt/g4-DM1 with gemcitabine in inhibition of xenograft PDAC growth. These findings provide the rationale for using Zt/g4-DM1 with chemotherapeutics as a novel and potential approach for PDAC therapy. We believe the results obtained from this preclinical study prove that the use of RON-targeted ADC is a suitable strategy for PDAC treatment, which lays the foundation for development of humanized anti-RON ADC for potential clinical trials.

Materials and methods

Cell lines and reagents

Panc-1, BxPC-3, DLD1, HT29, HCT116, H1993, and MDA-MB-231 cell lines were from American Type Cell Culture (ATCC, Manassas, VA). FG and L3.6pl cell lines were provided by Drs. A.M. Lowy (Department of Surgery, University of California at San Diego, CA) and G.E. Gallick (University of Texas M.D. Anderson Cancer Center, Houston, TX), respectively. Individual cell lines were cultured in their proper culture media supplemented with 10% of fetal bovine serum (FBS). Mouse anti-RON mAb Zt/f2 and

Anti-RON ADC for pancreatic cancer therapy

rabbit IgG antibody against the RON C-terminus (R#5029) were used as previously described [18]. Goat anti-mouse IgG labeled with fluorescein isothiocyanate (FITC) or rhodamine was from Jackson ImmunoResearch (West Grove, PA).

Preparation of Zt/g4-DM1

Zt/g4-DM1 and control mouse IgG (CmlgG)-DM1 with drug to antibody ratio of 3.9:1 and 4.1:1, respectively, were prepared as previously described [26]. Conjugates were purified, sterilized through a filter, and verified by hydrophobic interaction chromatography (HIC) as previously described [26].

Analysis of Zt/g4-DM1 plasma concentrations and pharmacokinetics

Female nude mice (five mice per group) received a single dose of Zt/g4-DM1 at 3, 10, 20 mg/kg through tail vein. Blood samples were collected at different time intervals. Plasma concentrations of Zt/g4-DM1 were determined using the DM1 ADC enzyme-linked immunosorbent assay (ELISA) kit (Eagle Biosciences Inc., Nashua, NH), which uses anti-DM1 antibody to measure DM1-antibody conjugates with the sensitivity of 0.024 µg per ml (www.eaglebio.com). The PK parameters were calculated using statistical software.

Immunofluorescence analysis of RON expression

The number of cell-surface RON was quantitatively determined by DAKO QIFKIT (www.dako.com). After establishing a calibration curve, the number of RON receptors on the cell surface was determined by interpolation following the manufacturer's instructions. Endocytic RON and cytoplasmic lysosomal-associated membrane protein (LPAM) 1 were detected by treating cells (1×10^5 cells per well in a 6-well plate) with 5 µg/ml Zt/g4-DM1 for 12 h. Antibodies specific to RON (Zt/f2) or LAMP1 were used followed by goat anti-mouse IgG coupled with fluorescein isothiocyanate (FITC) or rhodamine, respectively. Nuclear DNAs were stained with 4',6-diamidino-2-phenylindole (DAPI). Immunofluorescence was observed under Olympus BK71 microscope equipped with DSU/fluorescent apparatus.

Western blot analysis

Cellular proteins (50 µg per sample) were separated in an 8% or 12% SDS-PAGE under reduced conditions as previously described [18]. Western blot analysis of RON, cyclin-D1, poly ADP ribose polymerase (PARP), and caspase-3 fragments was performed using antibodies specific to corresponding proteins as previously described [18]. Membranes also were reprobbed with antibody to actin to ensure equal sample loading.

Flow cytometric analysis of cell cycle

PDAC cell lines (1×10^6 cells per dish) were incubated at 37°C with 5 µg/ml Zt/g4-DM1 for various times, labeled with propidium iodide, and then analyzed by an Accuri Flow Cytometer. Cell cycle changes were determined by measuring DNA contents as previously described [29].

Assays for cell viability and death

Cell viability 96 h after Zt/g4-DM1 treatment was determined by the 3-(4,5-dimethylthiazol-2-yl)-5-(3-carboxymethoxyphenyl)-2-(4-sulfophenyl)-2H-tetrazolium (MTS) assay [22]. Viable or dead cells were determined by the trypan blue exclusion assay. A total of 900 cells were counted from three individual wells to reach the percentages of dead cells.

Xenograft PDAC model and treatment with Zt/g4-DM1 and gemcitabine

All experiments on mice were approved by the TTUHSC institutional animal care committee. Male and female athymic nude mice aged 6-8 weeks (Taconic, Cranbury, NJ) were injected with 5×10^6 BxPC-3, FG, or L3.6pl cells in the subcutaneous space of the right flank as previously described [21, 26]. Mice were randomized into different groups (five mice per group). Treatment began when all tumors had a mean tumor volume of ~ 150 mm³. Mice received 10 or 20 mg/kg Zt/g4-DM1 in 0.1 ml PBS through tail vein in the Q8 \times 3 or Q12 \times 2 regimen. Gemcitabine was administered at 60 mg/kg in the Q4 \times 5 schedules. Tumor volumes were measured every four days according to a formula: $V = \pi/6 \times 1.58 \times (\text{length} \times \text{width})^{3/2}$ [26]. Animals were euthanized when tumor volumes exceeded 2000 mm³ or if tumors became necrotic or ulcerated through the skin.

Anti-RON ADC for pancreatic cancer therapy

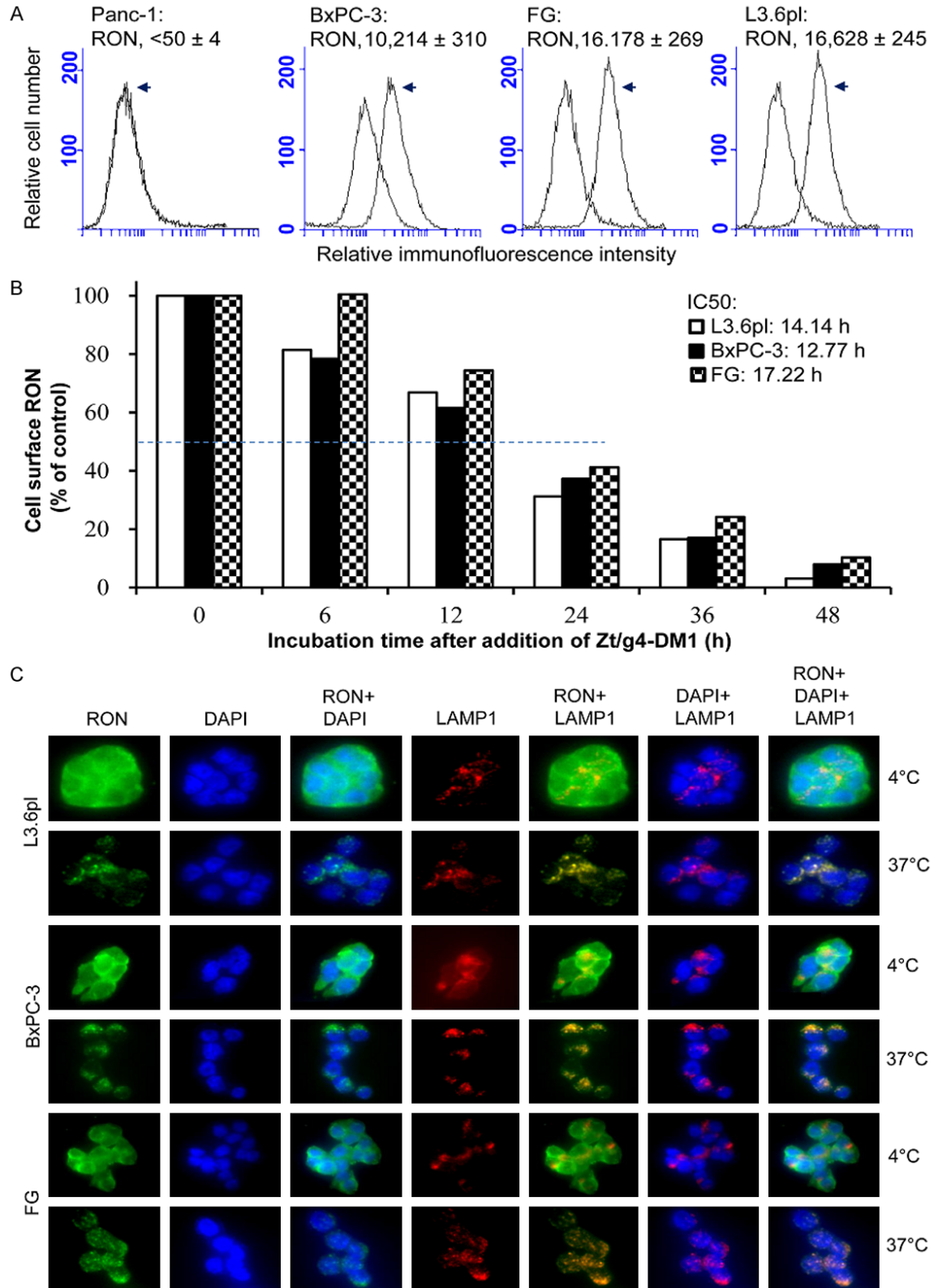


Figure 1. Induction of RON endocytosis by Zt/g4-DM1 in PDAC cell lines: (A) Levels of RON expression by PDAC cell lines. Four PDAC cell lines (1×10^6 cells/ml) in PBS were incubated at 4°C with 5 μ g/ml Zt/g4 for 60 min. Isotope matched mouse IgG was used as the control. Cell surface RON was quantitatively determined by immunofluorescence analysis using QIFKIT® (DAKO). (B) Kinetic reduction of cell surface RON. BxPC-3, FG and L3.6pl cells ($1 \times$

Anti-RON ADC for pancreatic cancer therapy

10^5 cells per dish) were treated at 37 °C with 5 µg/ml of Zt/g4-DM1, collected at different time points, washed with acidic buffer to eliminate cell surface bound IgG [22], and then incubated with 2 µg/mL of anti-RON mAb Zt/F2. Immunofluorescence was analyzed by flow cytometer using FITC-coupled anti-mouse IgG. Immunofluorescence from cells treated with Zt/g4-DM1 at 4 °C was set as 100%. Internalization efficiency (IC_{50}) was calculated as the time required to achieve the 50% reduction of cell surface RON. (C) Immunofluorescent localization of endocytic RON in cytoplasm. BxPC-3, FG, and L3.6pl cells (1×10^5 cells per chamber) were treated at 4 °C or 37 °C with 5 µg/ml of Zt/g4-DM1 for 12 h followed by FITC-coupled goat anti-mouse IgG. LAMP1 was detected using mouse anti-LAMP1 mAb and used as a marker for protein cytoplasmic localization. After cell fixation, immunofluorescence was detected using the BK70 Olympus microscope equipped with a fluorescence apparatus. DAPI was used to stain nuclear DNA. Images were also overlapped to show the co-localization of RON with LAMP1 in cytoplasm.

Statistical analysis

GraphPad 6 software was used for statistical analysis. Results are shown as mean \pm SD. The half maximal inhibitory concentration (IC_{50}) and half maximal effective concentration (EC_{50}) of Zt/g4-DM1 were calculated as previously described [26]. The data between control and experimental groups were compared using Student t test. Chi-squared analysis was used for correlational study. Isobolograms were used for analysis of synergism in drug combination studies. Statistical differences at $p < 0.05$ were considered significant.

Results

Overexpression renders RON a suitable target for anti-RON ADC-directed drug delivery

Four human PDAC cell lines expressing variable levels of RON were selected as the ADC delivering/targeting model (**Figure 1A**). These cell lines have been previously used to determine the role of RON in regulating PDAC tumorigenic activity [7-17]. For quantitative analysis, we first determined the number of RON molecules on the cell surface using DAKO immunofluorescence QIFKIT as previously described [26]. The calculated RON molecules per PDAC cell were $10,214 \pm 310$ for BxPC-3, $16,178 \pm 269$ for FG, and $16,628 \pm 245$ for L3.6pl. Specific binding was not observed in Panc-1 cells ($< 50 \pm 4$), which will serve as the negative control.

We studied Zt/g4-DM1-induced RON endocytosis, a process essential for delivering DM1 into PDAC cells. Zt/g4-DM1 was generated by conjugation of Zt/g4 (IgG1a/ κ) with DM1 via thioether linkage with a drug-antibody ratio of 3.8:1 [26]. Zt/g4-DM1 caused a progressive reduction of RON in a time-dependent manner in all three PDAC cell lines tested (**Figure 1B**). Less than 20% of RON remained on the cell surface after a 48 h treatment. The time required for

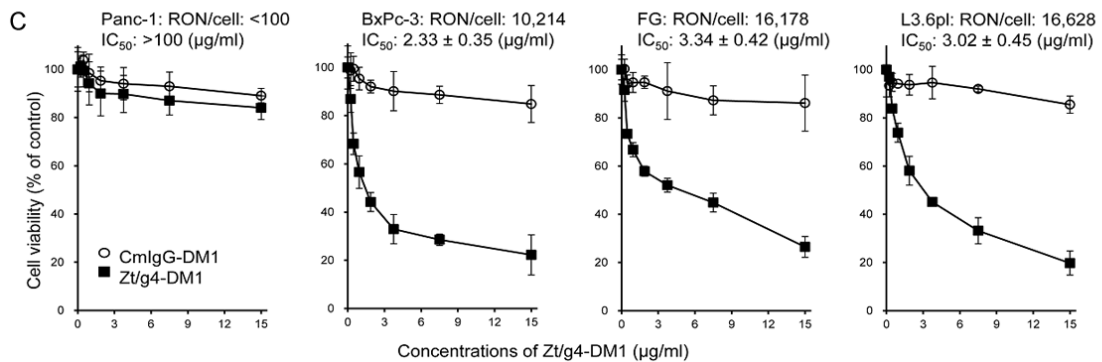
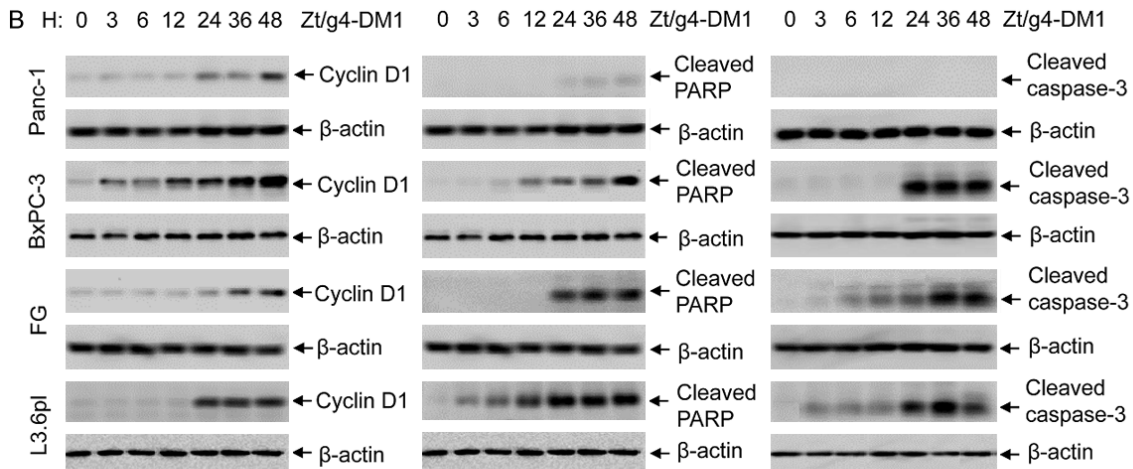
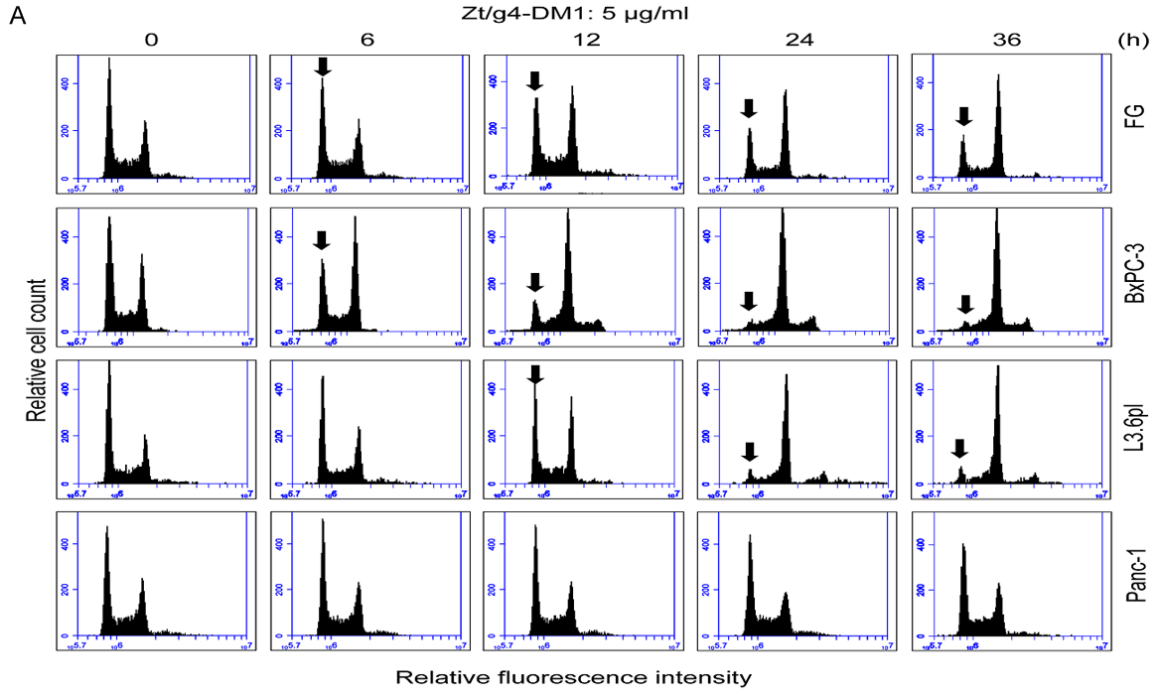
Zt/g4-DM1 to induce 50% RON reduction (internalization efficacy) was 14.14 h, 12.77 h, and 17.22 h for L3.6pl, BxPC-3, and FG, respectively. No statistically differences among three PDAC cell lines were observed. Thus, Zt/g4-DM1 is effective in induction of RON endocytosis by PDAC cells.

We further confirmed Zt/g4-DM1-induced RON endocytosis by immunofluorescence analysis of endocytic RON in cytoplasm in three PDAC cell lines (**Figure 1C**). Cells stained for LAMP1 were used as a marker for co-localization. RON was detected on the cell surface at 4°C. The intracellular localization of endocytic RON occurred at 37°C after Zt/g4-DM1 treatment. The endocytic RON was co-localized with LAMP1 within lysosomes. Thus, cell surface RON is internalized and endocytic RON localizes in cytoplasm following Zt/g4-DM1 treatment.

Anti-RON ADC in vitro inhibits PDAC cell growth and causes massive cell death

Functional analysis showed that Zt/g4-DM1 treatment results in PDAC cell cycle changes, featuring a significant reduction in G0/G1 phase, a decrease in S phase, and a dramatic increase in G2/M phase (**Figure 2A**). The time required for Zt/g4-DM1 to induce a 50% reduction in G0/G1 phase was 10.33, 14.04, and 13.75 hours for BxPC-3, FG, and L3.6pl, respectively (**Table 1**). Quantitative measurement of cell cycle changes at 24 h is shown in **Table 2**. We also analyzed cyclin D1 expression, which plays a role in regulating G1 to S phase progression [31]. Results from Western blotting of cell lysates revealed that Zt/g4-DM1 dramatically induces cyclin D1 expression in a time-dependent manner in RON expressing PDAC cell lines (**Figure 2B**). In contrast, this effect was minimal on RON-negative PDAC Panc-1 Cells. Thus, results in **Figure 2A** and **2B** demonstrate that Zt/g4-DM1 treatment has a significant effect on cell cycles in PDAC cells.

Anti-RON ADC for pancreatic cancer therapy



Anti-ROn ADC for pancreatic cancer therapy

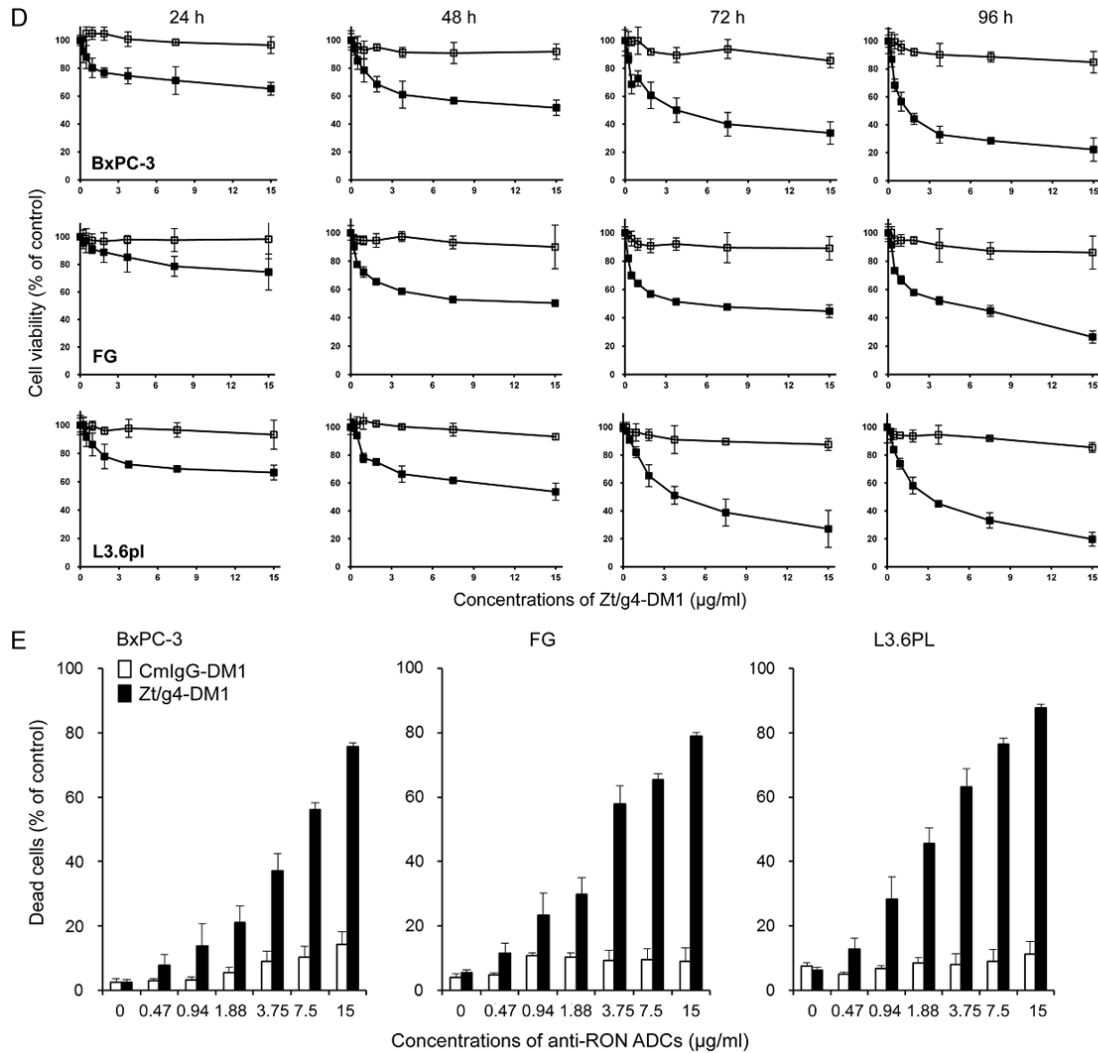


Figure 2. Effect of Zt/g4-DM1 on cell cycle, viability, and death by PDAC cell lines expressing different amounts of cell surface RON: (A) Changes in cell cycles. Three PDAC cell lines (1×10^6 cells per dish in 10% DMEM with 10% FBS) were treated at 37°C with $5 \mu\text{g/ml}$ of Zt/g4-DM1 for various times, collected, stained with propidium iodide, and then analyzed by flow cytometer [26]. A decrease in G1 phase and an increase in G2/M phases are marked with arrows. (B) Cyclin D1 expression and PARP/caspase-3 cleavage. PDAC cell lines (3×10^6 cells per dish) were treated with $5 \mu\text{g/ml}$ Zt/g4-DM1 for various times. Western blot analysis of cellular proteins ($50 \mu\text{g}$ /per lane) was performed using antibodies specific to cyclin-D1, cleaved PARP, or cleaved caspase-3, respectively. Actin was used as the loading control. (C) Effect of Zt/g4-DM1 on viability of PDAC cells expressing different levels of RON. Four PDAC cell lines (8000 cells per well in a 96-well plate in triplicate) were treated with different amounts of Zt/g4-DM1 for 96 h. Cells treated with normal mouse IgG conjugated with DM1 (CmlgG-DM1) serviced as the control. Cell viability was determined by the MTS assay. (D) Kinetic effect of Zt/g4-DM1 on cell viability. Zt/g4-DM1 treatment of PDAC cells was performed as described in (C). Cell viability was determined at different intervals by the MTT assay. (E) Death of PDAC cells after Zt/g4-DM1 treatment. PDAC cells were treated with different amounts of Zt/g4-DM1 for 96 h. The percentages of cell death were determined by the trypan blue exclusion method.

We next studied the effect of Zt/g4-DM1 on cell viability. Sensitivity of PDAC cells to free DM1 is shown in [Supplementary Figure 1](#) with IC_{50} at 6.64, 2.07, 2.25, and 4.69 nM for Panc1, BxPC-3, FG, and L3.6pl cells, respectively ([Table 1](#)). These results indicate that the four PDAC cell

lines are highly sensitive to DM1. Treatment of PDAC cells with Zt/g4-DM1 resulted in a significant reduction in cell viability in time and dose-dependent manners ([Figure 2C, 2D](#)). The IC_{50} values at 96 h were 2.33 ± 0.35 , 3.34 ± 0.42 , and $3.02 \pm 0.45 \mu\text{g/ml}$ Zt/g4-DM1 (equivalent

Anti-RON ADC for pancreatic cancer therapy

Table 1. Efficacy of Anti-RON ADC Zt/g4-DM1 in vivo in Regulating Cell Cycle, Viability, and Death of Pancreatic Cancer Cell lines*

Human PDAC cell lines	RON receptor per cell	IC ₅₀ values of free DM1 (nM)	EC50 values of Zt/g4-DM1 in PDAC cells			
			Endocytosis of RON (h)	G1/G0 Phase Change (h)	Cell Viability (µg/ml)	Cell Death (µg/ml)
Panc-1	< 100	6.64 ± 1.07	ND	ND	> 100	ND
BxPC-3	10,214 ± 310	2.07 ± 0.37	12.77	10.33	2.33 ± 0.35	5.63 ± 0.21
FG	16,178 ± 269	2.25 ± 0.24	17.22	14.04	3.34 ± 0.42	3.27 ± 0.43
L3.6pl	16,628 ± 245	4.69 ± 0.64	14.14	13.75	3.02 ± 0.45	2.24 ± 0.18
Average	14,340 ± 3580	3.91 ± 1.47	14.71 ± 2.28	12.71 ± 2.06	2.95 ± 1.03	3.37 ± 1.34

*Individual PDAC cell lines were used to determine RON expression, cellular sensitivity to free DM1, Zt/g4-DM1-induced RON internalization, cell cycle change, cell viability, and cell death as detailed in Materials and Methods.

Table 2. Induction of cell cycle changes by anti-RON ADC Zt/g4-DM1 in pancreatic cancer cell lines*

PDAC cell lines	Changes of cells cycles after Zt/g4-DM1 treatment (%)													
	G0/G1 phase				S phase				G2M phase				Polyploidy	
	0 h	12 h	24 h	36 h	0 h	12 h	24 h	36 h	0 h	12 h	24 h	36 h	0 h	36 h
L3.6pl	45.24	33.91	8.55	7.59	23.25	26.01	16.44	22.45	23.58	34.01	53.34	54.05	7.93	14.95
BxPc-3	44.58	24.55	7.05	7.03	21.31	14.09	16.00	15.73	31.51	50.06	61.39	62.36	2.61	14.85
FG	42.23	31.73	26.01	22.48	21.92	20.65	18.15	17.14	27.49	36.85	46.31	50.74	8.36	9.64
Average	44.02	30.06	13.87	12.16	22.16	20.25	16.86	18.44	27.53	40.31	53.68	55.73	6.30	13.15
	± 1.58	± 4.90	± 10.5	± 8.76	± 0.99	± 5.97	± 1.14	± 3.54	± 3.97	± 8.57	± 7.55	± 6.00	± 3.20	± 3.04

*Individual PDAC cell lines were treated with 5 µg/ml of Zt/g4-DM1 for various time intervals followed by flow cytometric analysis to determine their cell cycles as previously described [16].

to 120, 54, and 63 nM of free DM1) for BxPC-3, FG, and L3.6pl cells, respectively (**Table 1**). The Effect of Zt/g4-DM1 was minimal on Panc-1 cells with estimated IC₅₀ values at: 100 µg/ml. These results indicate that Zt/g4-DM1 is effective in reduction of PDAC cell viability.

Morphological observation indicated a massive cell death 96 h after Zt/g4-DM1 treatment (**Supplementary Figure 2**). Quantitative analysis of cell death induced by Zt/g4-DM1 is shown in **Figure 2E** with IC₅₀ values ranging from 5.63, 3.27, and 2.24 µg/ml for BxPC-3, FG and L3.6pl cells (**Table 1**), respectively. Analysis of cellular proteins further confirmed that the Zt/g4-DM1 treatment results in cleavage of PARP and Caspase-3, two indicators of apoptotic cell death (**Figure 2B**). Thus, Zt/g4-DM1 *in vitro* is able to induce apoptotic death of PDAC cells in a dose-dependent manner.

Levels of RON Expression correlates *in vitro* with efficacy of anti-RON ADC Zt/g4-DM1

To address the relationship between the Zt/g4-DM1 efficacy and the number of cell surface RON receptors, we collected PDAC, colon, lung, and breast cell lines expressing variable levels of RON and tested their response to Zt/g4-DM1

for viability IC₅₀ values. A direct correlation was established by plotting the individual IC₅₀ values against the cell surface number of the RON receptor (**Figure 3**). We conclude that the minimal number of cell-surface RON molecules required for Zt/g4-DM1 to achieve the 95% reduction in cell viability (EC₉₅) is around 10,000 receptor molecules per cell. A decrease in the level of RON correlated proportionally with the diminished efficacy of Zt/g4-DM1. Thus, PDAC cells expressing ~10,000 RON molecules on cell surface per cell are required for Zt/g4-DM1 *in vitro* to show the maximal efficacy.

Pharmacokinetic analysis models the efficacy of Zt/g4-DM1 *in vivo* in inhibition of xenograft PDAC growth

The PK of Zt/g4-DM1 was studied in tumor-bearing and nonbearing mice to determine the time-dose relationship of Zt/g4-DM1. Since Zt/g4 cross-reacted with mouse homologue of RON with similar binding affinity, we wanted to know: a) any alterations in Zt/g4-DM1 PK in tumor-bearing mice and b) RON-dependent behavior of Zt/g4-DM1 in tumor-nonbearing mice. Blood samples were collected at different time intervals. DM1-coupled Zt/g4 was mea-

Anti-RON ADC for pancreatic cancer therapy

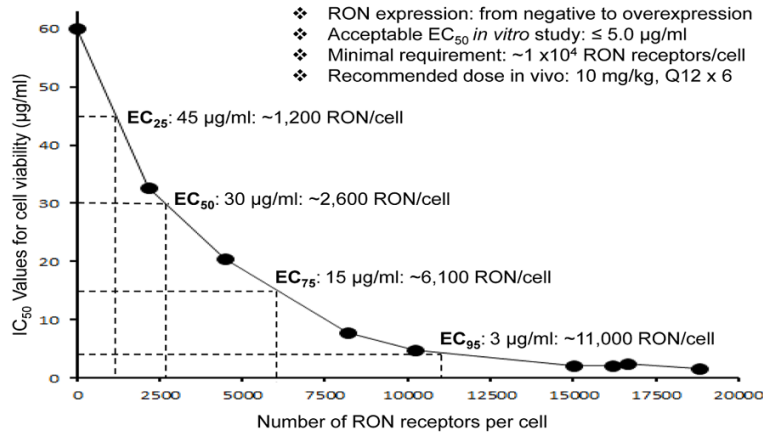


Figure 3. Correlation between RON receptor and Zt/g4-DM1 efficacy: Cell viability IC₅₀ values from a panel of cancer cell lines expressing different levels of RON per cell (Panc-1: < 10; H1993: 2,152; DLD1: 4,480; MDA-MB-213: 8,185; BxPC-3: 10,214; HCT116: 15,005; FG: 16,178; L3.6pl: 16,628; and HT29: 18,793) were plotted with different numbers of RON expressed per cell. Zt/g4-DM1 at the amount below 5 mg/ml to achieve an IC₅₀ value was used as the effective dose to determine the required receptor number to reach the EC₉₅ value. The IC₅₀ values for cell viability or death at 96 h from individual groups were calculated using the GraphPad Prism 6 software. Results shown here are from one of three experiments with similar results.

sured using a DM1 antibody ELISA kit (Eagle Biosciences, Inc., Nashua, NH). Results in **Figure 4A** show serum concentrations of Zt/g4-DM1 in a two-compartment model with several parameters in both tumor-bearing mice injected with a single dose of Zt/g4-DM1 at 3 and 10 mg/kg and in tumor-nonbearing mice injected with a single dose of 20 mg/kg Zt/g4-DM1. A dose-proportional increase in Zt/g4-DM1 plasma concentrations with increasing dose from 3 to 20 mg/kg was observed. Overall, the data from tumor-bearing mice were overlapped with those from the tumor-nonbearing mice with 95% prediction intervals. By calculation, the mean plasma clearance was 0.22 ml/day/kg and the terminal half-life ($t_{1/2\beta}$) was 6.01 days. Thus, the PK of Zt/g4-DM1 is in no difference between tumor-bearing and nonbearing mice, suggesting that tumor growth does not affect the dynamics of Zt/g4-DM1. Moreover, RON expression by tumor cells has no impact on Zt/g4-DM1 disposition *in vivo*.

A time-dose relationship using the PK parameters was established to predict the effectiveness of Zt/g4-DM1 in the xenograft tumor model. We first projected a target dose of Zt/g4-DM1 required to achieve a balance between tumor growth and inhibition (tumorigenic concentration, TSC) for the xenograft growth of

CRC HT29 and SW620 cells [26]. The PK parameters predicted Zt/g4-DM1 at 5 mg/kg as the TSC to cause tumorigenesis (**Figure 4B**). For the BxPC-3 xenograft tumor model, the projected TSC was 3.02 mg/kg according to the terminal half-life of Zt/g4-DM1 (**Figure 4C**). Since a single dose of Zt/g4-DM1 at 60 mg/kg is toxic in mice [26], we reasoned that Zt/g4-DM1 at 20 mg/kg in the Q12 x 2 or at 10 mg/kg in the Q8 x 3 schedule should be effective in inhibition of xenograft PDAC growth *in vivo*.

Zt/g4-DM1 is effective in vivo in inhibition of xenograft PDAC growth and in depletion of RON expressing PDAC cells

The efficacy of Zt/g4-DM1 at 20 mg/kg in the Q12 x 2 regimen was first applied to PDAC xenograft models initiated by BxPC-3, FG, and L3.6pl cells. The growth of BxPC-3 xenografts was relatively slow but tumors were highly sensitive to Zt/g4-DM1-mediated inhibition (**Figure 5A**). More than 90% inhibition was achieved at day 32 as determined by calculating average tumor weights (0.73 ± 0.33 versus 0.06 ± 0.03) (**Figure 5B**). It is worth noting that the significant regrowth of tumors was not observed up to day 32.

Both FG and L3.6pl cell-initiated tumors were fast growing with tumor volumes reaching ~2,000 mm³ within 16 days after cell inoculation (**Figure 5A**). FG xenograft tumors were initially sensitive to Zt/g4-DM1 with more than 85% inhibition of tumor volume at day 20 (**Figure 5A**). However, the efficacy of the second dose was dramatically diminished with increased tumor regrowth. Nonetheless, after growth for additional 12 days, at day 32, the average weight of Zt/g4-DM1-treated FG xenografts (1.89 ± 0.56) still was ~25% less than that of the control tumors (2.49 ± 0.80) collected at day 20 (**Figure 5B**).

The efficacy of Zt/g4-DM1 in L3.6pl xenograft tumors was moderate with an average 76%

Anti-RON ADC for pancreatic cancer therapy

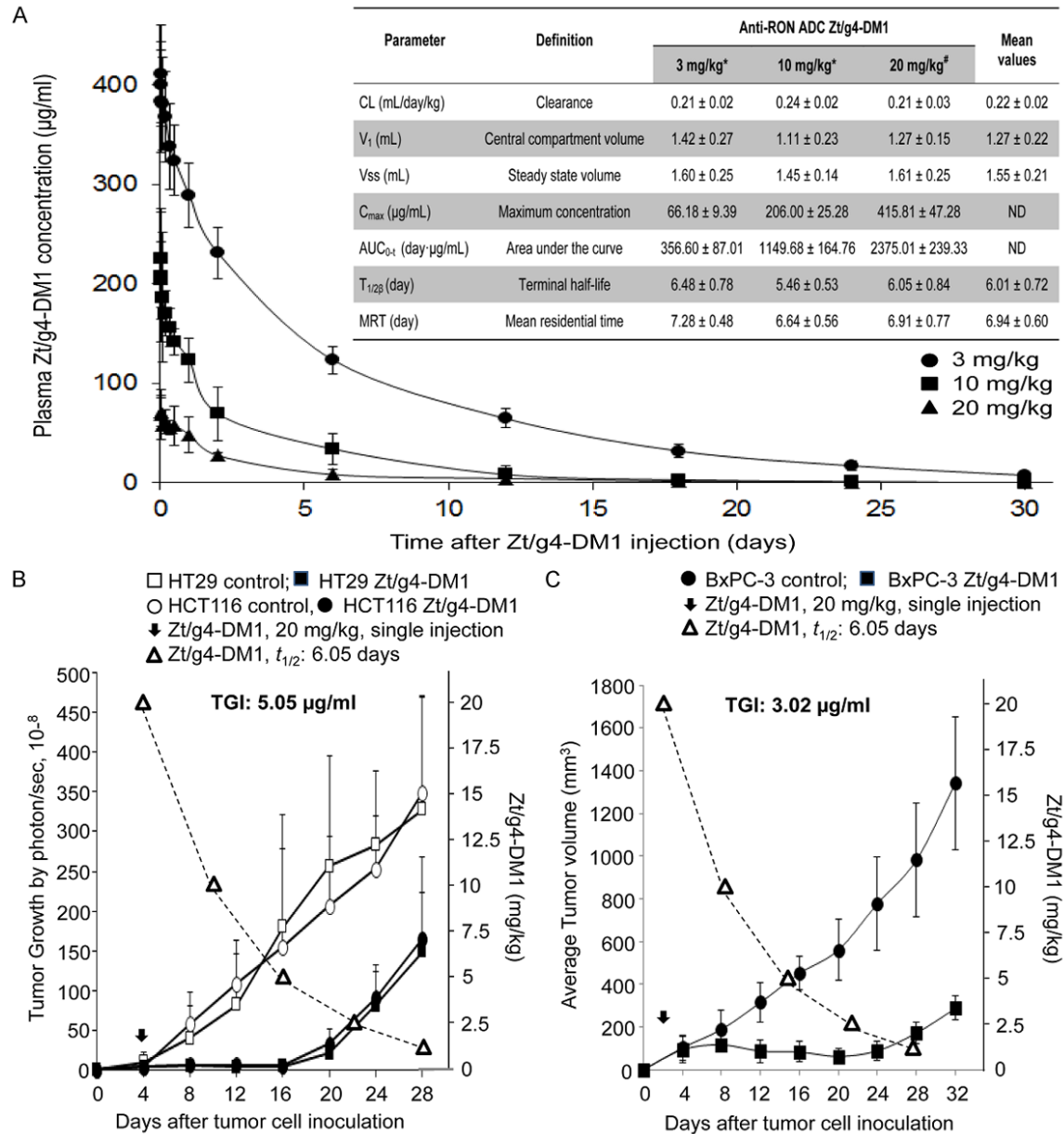
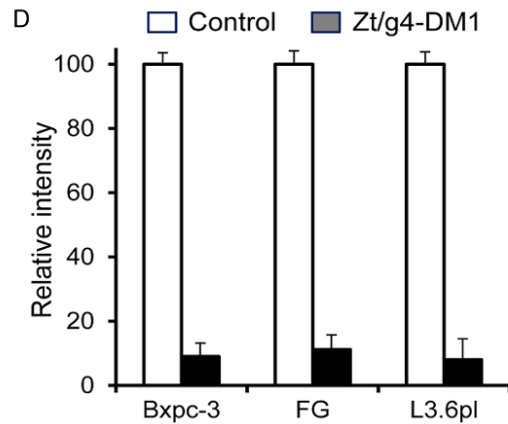
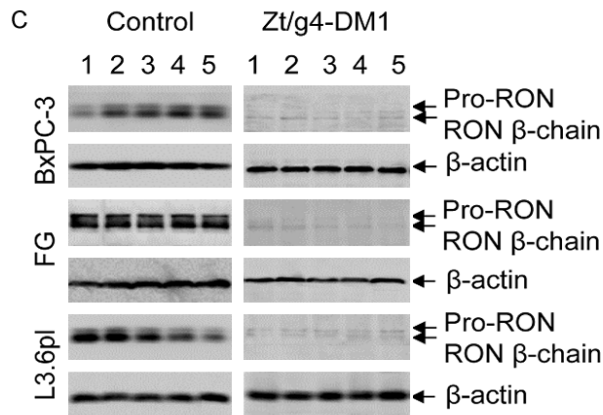
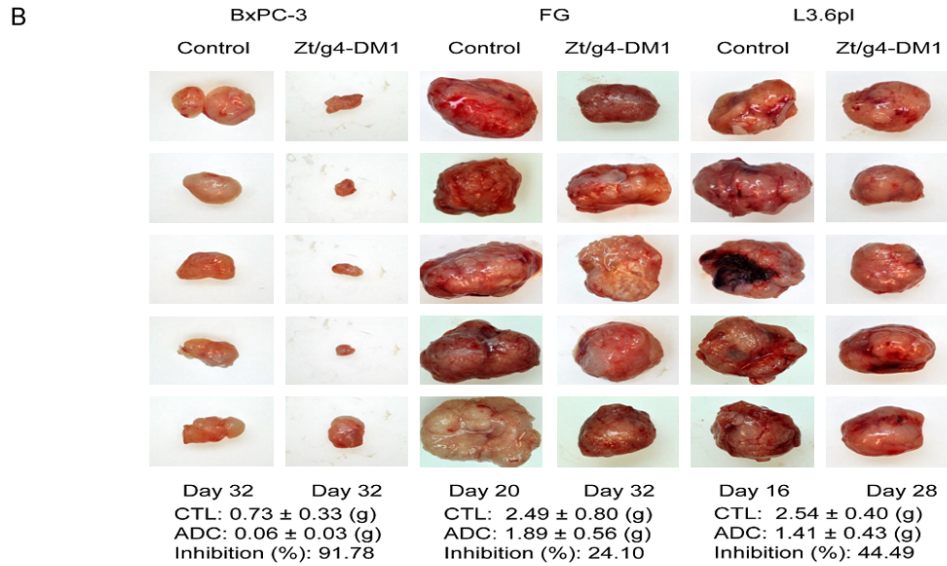
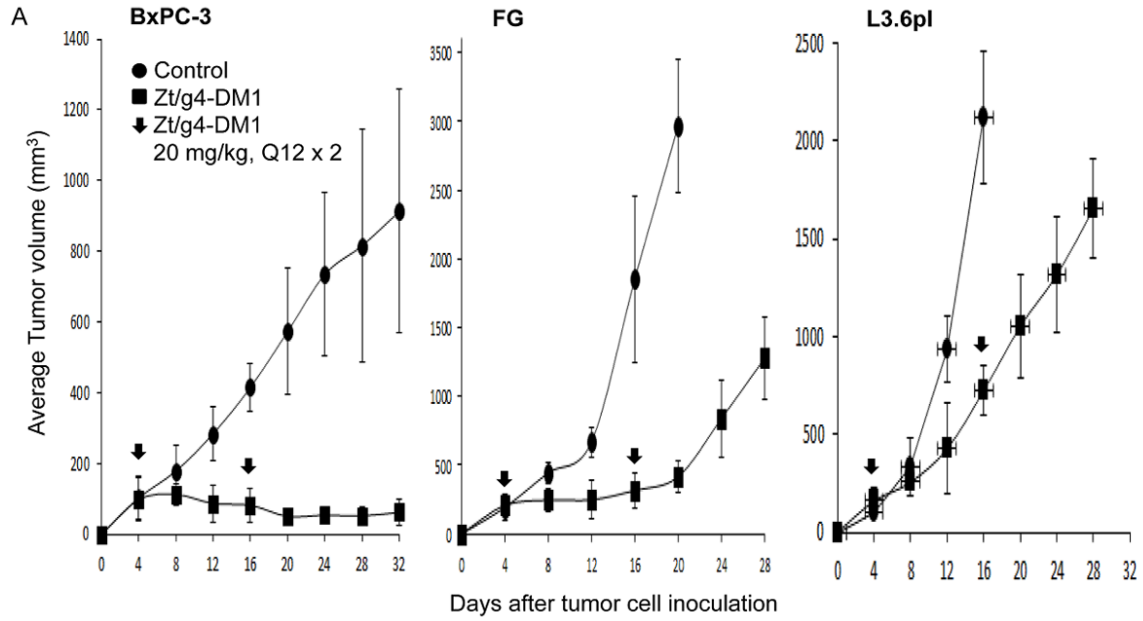


Figure 4. Analysis of pharmacokinetics of Zt/g4-DM1 for predicting the time-dose-relationship: Tumor-bearing and -nonbearing mice (athymic nude, 5 mice per group) were injected with a single dose of Zt/g4-DM1. Collected blood samples were analyzed using the DM1 antibody ELISA kit (Eagle Biosciences, Inc., Nashua, NH) to determine the amount of DM1-coupled Zt/g4 in plasma. Various PK parameters were calculated using the software provided by Eagle Biosciences. (A): PK from both tumor-bearing and nonbearing mice injected with a single dose of 3, 10, and 20/mg/kg Zt/g4-DM1. (B) Dynamics of Zt/g4-DM1 *in vivo* plotted with the growth curve of CRC xenograft tumors. Athymic nude mice were inoculated with HT29 and HCT116 cells (5×10^5 cells per mouse, five mice per group). A single dose of Zt/g4-DM1 at 20 mg/kg was injected when tumor volume reached ~ 150 mm³. PK data from (A) was plotted to the tumor growth curve. (C) Dynamics of Zt/g4-DM1 *in vivo* plotted with the growth curve of BxPC-3 xenograft tumors. Mice bearing BxPC-3 xenograft tumors were injected with a single dose of Zt/g4-DM1 at 20 mg/kg through tail vein when tumor volume reached ~ 150 mm³. PK data from (A) was plotted to the tumor growth curve. TSCs for CRC and PDAC xenograft models were determined as the minimal dose of Zt/g4-DM1 required to balance tumor growth and inhibition.

reduction in tumor volume at day 16 (**Figure 5A**). The effect of the second dose appeared to

be minimal as evident by an accelerated phase of tumor regrowth at a rate similar to that of

Anti-RON ADC for pancreatic cancer therapy



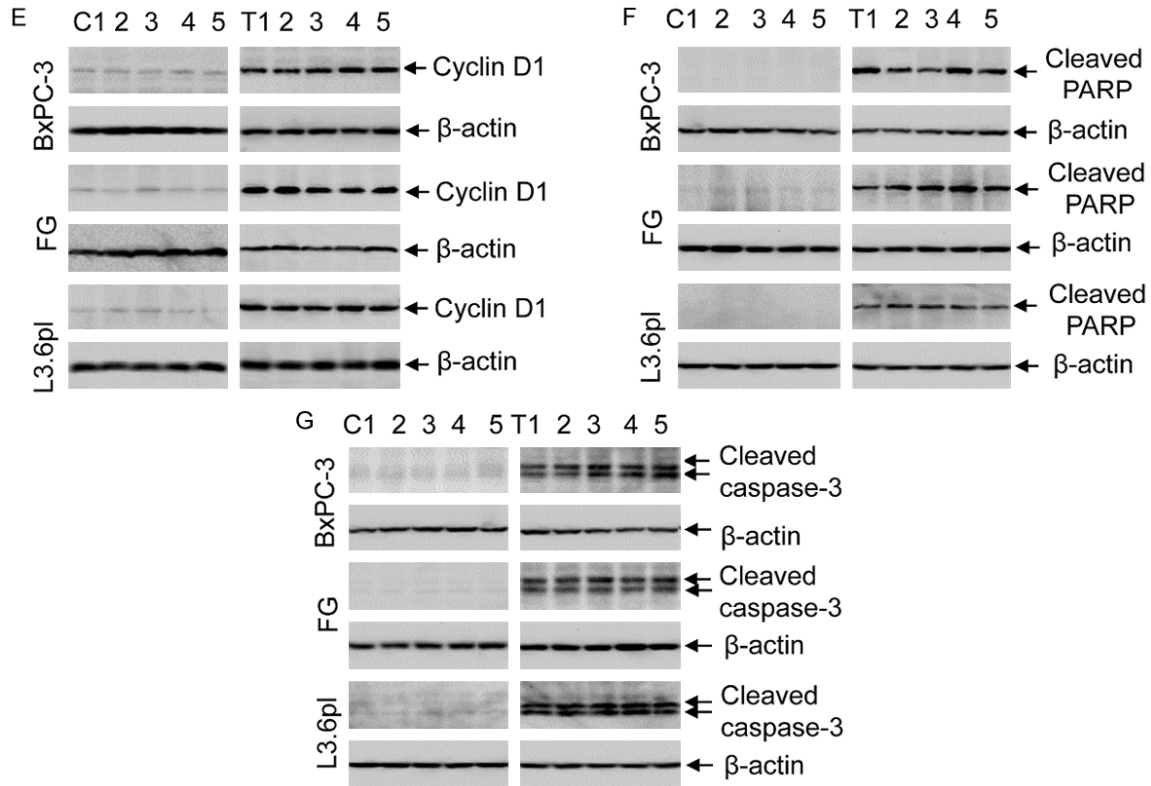


Figure 5. Therapeutic efficacy of Zt/g4-DM1 in three PDAC xenograft tumor models: (A) Athymic nude mice (five mice per group) were subcutaneously inoculated with 5×10^6 BxPC-3, FG, and L3.6pl cells and tumors were allowed to reach an average volume of $\sim 150 \text{ mm}^3$. Zt/g4-DM1 at 20 mg/kg was injected through tail vein in the Q12 \times 2 regimen. Mice injected with CmlgG-DM1 were used as the control. Tumor volume was measured every four days using a method previously described [26]. Mice were euthanized when tumor volume reached $\sim 1000 \text{ mm}^3$ (for BxPC-3 model) or 2000 mm^3 (for FG and L3.6pl models). The percentages of tumor growth inhibition were calculated by a formula: $100\% - (\text{average tumor volume from treatment group}) / (\text{average tumor volume from control group}) \times 100\%$. (B) Individual tumors from different groups were collected from euthanized mice. The percentages of inhibition were calculated by a formula: $100\% - (\text{average tumor weight from treatment group}) / (\text{average tumor weight from control group}) \times 100\%$. (C) A portion of tumor samples from different groups were lysed using the tissue lysis buffer as previously described [26]. Proteins ($50 \mu\text{g}$ per sample) were subjected to Western blot analysis to detect RON using rabbit anti-RON IgG antibody #5029 [18]. (D) Densitometry analysis was performed to determine the levels of RON expression by individual samples using the software from the BioRad 5000 Image system. Expression of cyclin-D1 (E), cleaved PARP (F) and caspase-3 (G) by individual tumors after Zt/g4-DM1 treatment was determined by Western blot analysis of tumor lysate using antibodies specific to corresponding proteins as described in (C).

control tumors. However, the average tumor weight from Zt/g4-DM1-treated tumors ($1.41 \pm 0.43 \text{ g}$) at day 28 remained $\sim 45\%$ less than that from the control tumors ($2.54 \pm 0.40 \text{ g}$) at day 16 (Figure 5B). Thus, Zt/g4-DM1 has an impact on the growth of L3.6pl xenograft tumors with a growth delay in more than 12 days.

Analysis of lysate proteins from PDAC xenograft tumors confirmed that RON expression was significantly diminished in xenograft tumors derived from all three PDAC cell lines. The average reduction measured 90.8%, 88.4%, and

87.7% for BxPC-3, FG, and L3.6pl xenograft tumors, respectively, in comparison with that of control tumors (Figure 5C, 5D). These results suggest that the majority of RON-expressing PDAC cells were eliminated. The remaining tumors were comprised of PDAC cells expressing no or low levels of RON. Thus, Zt/g4-DM1 effectively eliminates RON-expressing PDAC cells *in vivo*.

Results from Western blot analysis also confirmed cell cycle change in Zt/g4-DM1-treated tumor samples (Figure 5E). Cyclin-D1 expression was low in control tumors but increased

Anti-RON ADC for pancreatic cancer therapy

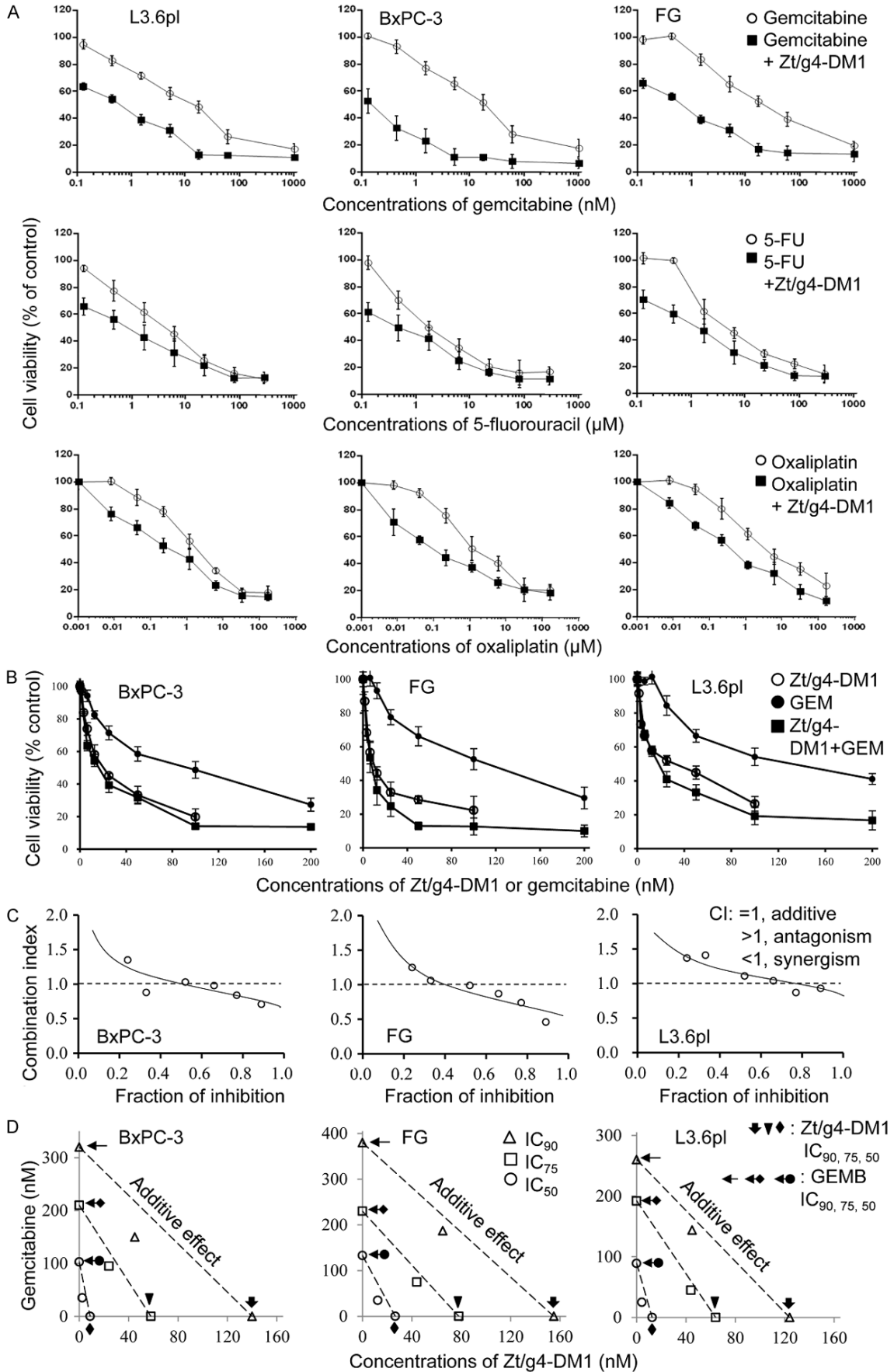


Figure 6. Synergistic effect of Zt/g4-DM1 in combination with chemotherapeutics *in vitro* on PDAC cell viability: (A) PDAC cell lines BxPC-3, FG, and L3.6pl cells (8,000 cell per well in a 96-well plate in triplicate) were cultured in DMEM with 10% FBS and treated with Zt/g4-DM1 at individual IC_{50} dose with or without different amounts of gemcitabine, oxaliplatin, or 5-FU for 96 h. Cell viability was measured using the MTT assay. Viability from control cells was defined as 100% and used to calculate percentages of cell viability for drug-treated cells. (B) Three PDAC cell lines were cultured as described above. Cells were treated with Zt/g4-DM1 (0.31 to 20 mg/ml, equivalent to 2 to 133 nM of free DM1), gemcitabine (2.5 to 160 nM) or their combination to form a fixed ratio of Zt/g4-DM1: gemcitabine at 1:1.2. The percentages of cell viability were calculated at 96 h as described above. (C) The percentages of cell viability from individual samples were calculated, converted, and then used for the fraction of inhibition-combination index (CI) plot as previously described [33]. (D) Results from (B) also were used for isobologram analysis to determine the IC_{50} , IC_{75} and IC_{90} values to define the synergism as previously described [33, 34]. Data shown here are from one of three experiments with similar results.

significantly in the Zt/g4-DM1-treated tumors, indicating cell cycle alterations *in vivo*. In addition, apoptosis was observed by the appearance of cleaved PARP fragments in Zt/g4-DM1-treated tumors but not in control samples (**Figure 5F**), indicating the cell death occurs after Zt/g4-DM1 treatment. Additional evidence for apoptosis was the detection of cleaved caspase-3 fragments in all Zt/g4-DM1-treated tumors but not in control groups (**Figure 5G**). Thus, Zt/g4-DM1 treatment alters cell cycle and causes apoptotic cell death in PDAC xenograft tumors.

Zt/g4-DM1 in combination with chemotherapeutics exerts an increased effect both in vitro and in vivo on PDAC cells

The differential efficacies of Zt/g4-DM1 in three PDAC xenograft tumor models prompted us to use a combinational therapy strategy to achieve the maximal efficacy. We first studied the effect of Zt/g4-DM1 at the IC_{50} dose *in vitro* in combination with three chemotherapeutics currently used for PDAC treatment. Results in **Figure 6A** show that cell viability was further reduced in all combination groups compared to the corresponding control groups. Thus, Zt/g4-DM1 shows the increased effect when combined with gemcitabine, oxaliplatin, or 5-fluorouracil (5-FU) in reduction of PDAC cell viability.

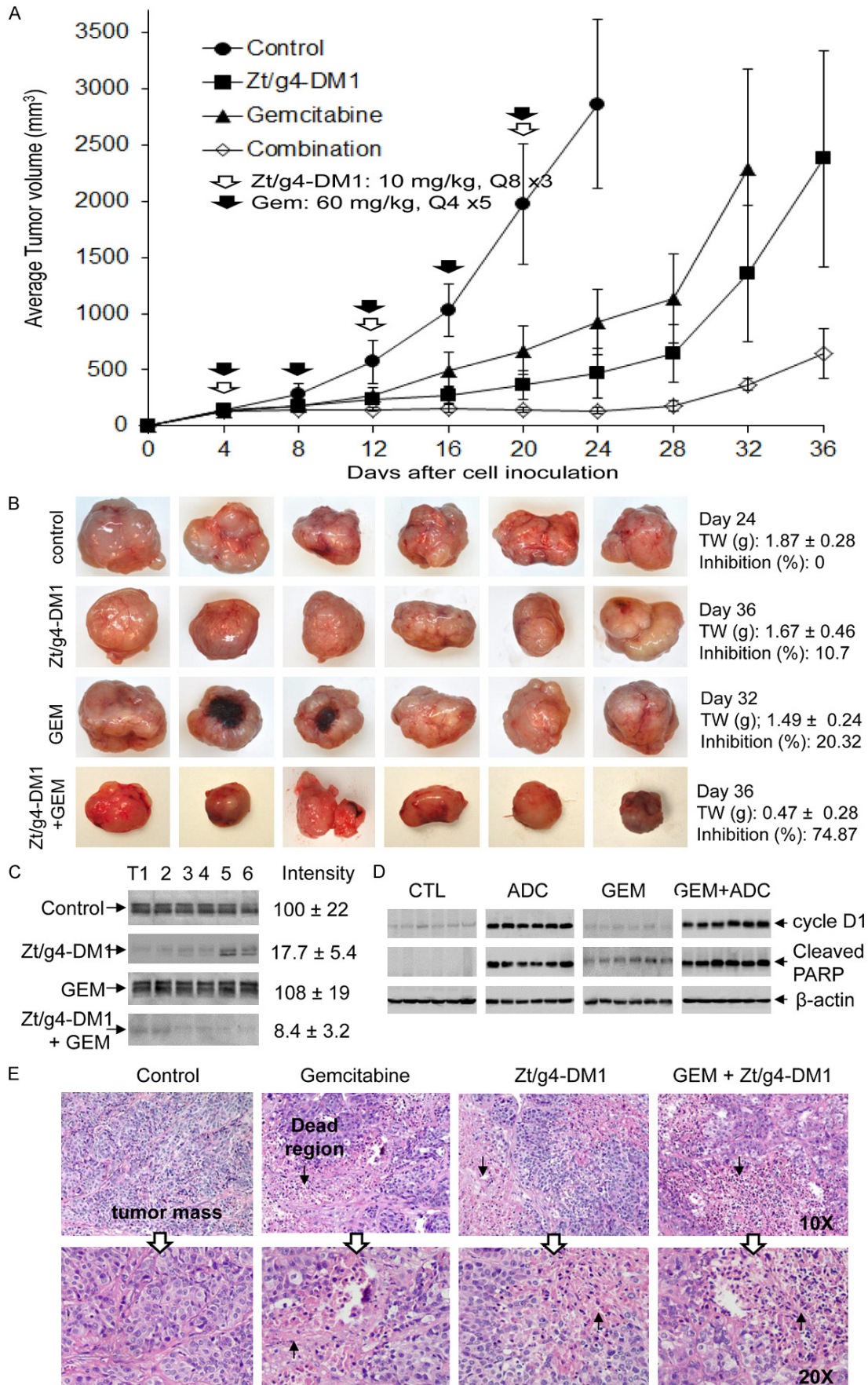
This increase in reduction of cell viability was further verified by combining Zt/g4-DM1 from 0.31 to 20 μ g/ml (equivalent to 2.02 to 133.34 nM of DM1) with gemcitabine from 2.5 to 160 nM to reach a fixed ratio of 1 to 1.2 (**Figure 6B**). The obtained data were then analyzed by plotting the fraction of inhibition against the combination index (CI) (**Figure 6C**) and by performing isobolograms to define IC_{50} , IC_{75} , and IC_{90} values (**Figure 6D**) [33, 34]. Results from these analyses confirmed the synergism between Zt/

g4-DM1 and chemotherapeutics when both drugs were used at the defined ratio.

We further confirmed the increase in tumor inhibition between Zt/g4-DM1 and gemcitabine combination in the FG xenograft model (**Figure 7A**). Zt/g4-DM1 at 10 mg/kg in a Q8 \times 3 regimen was combined with gemcitabine at 60 mg/kg in a Q4 \times 5 schedule. As expected, gemcitabine alone partially inhibited the growth of FG xenograft tumors with an average 67% reduction in tumor volume at day 24. Tumor regrowth was observed at day 20 even though the drug was continually administered. Similarly, Zt/g4-DM1 at 10 mg/kg partially delayed tumor growth with an average 85% reduction in tumor volume at day 20 followed by increased tumor regrowth. The combination therapy resulted in a complete inhibition of FG xenograft growth up to day 28. Moreover, tumor regrowth was further delayed up to day 32. Measurement of tumor weights at the end of the study revealed that the average tumor weight from the combined treatment groups at day 36 (0.47g \pm 0.28) was significantly less than that of the control group at day 24 (1.87 g \pm 0.28), from single Zt/g4-DM1 (1.67 g \pm 0.46) at day 36, and gemcitabine (1.49 g \pm 0.24) treated groups at day 32 (**Figure 7B**). These results suggest that the combination of Zt/g4-DM1 with gemcitabine has the increase in inhibition of the FG xenograft tumor growth.

We also used Western blot analysis of tumor lysate proteins to determine the combination effect on reduction of RON-expressing PDAC cells, changes in cell cycle, and appearance of apoptotic cells in tumor masses (**Figure 7C, 7D**). RON expression in FG-xenograft tumor lysates was significantly reduced after treatment with Zt/g4-DM1 or in combination with gemcitabine, consistent with those from *in vitro* studies (**Figure 5C**). As expected, gemcitabine

Anti-RON ADC for pancreatic cancer therapy



Anti-RON ADC for pancreatic cancer therapy

Figure 7. Synergism between Zt/g4-DM1 and gemcitabine *in vivo* in inhibition of xenograft PDAC growth: (A) Athymic nude mice (five mice per group) were subcutaneously inoculated with 5×10^6 FG cells to allow tumor growth to reach an average volume at $\sim 150 \text{ mm}^3$. Zt/g4-DM1 at 10 mg/kg was injected through tail vein in a Q8 \times 3 regimen. Mice injected with CmlgG-DM1 were used as the control. Gemcitabine was injected into the intraperitoneal cavity at 60 mg/kg in a Q4 \times 5 schedule. Both drugs were used for the combination group according to their own dose and schedule. Tumor volume was measured every four days. The percentages of tumor growth inhibition were calculated from the average tumor volume as described in **Figure 5A**. (B) Individual tumors from different groups were collected from euthanized mice when their volumes reached $\sim 2,000 \text{ mm}^3$ and then weighed to obtain the average tumor weight (gram). The percentages of inhibition were calculated as described in **Figure 5B**. (C) A portion of tumor samples from different groups were lysed using the tissue lysis buffer as previously described [26]. Lysate proteins (50 μg per sample) were subjected to Western blot analysis to detect RON using rabbit anti-RON IgG antibody #5029. Densitometry analysis was performed to determine the level of RON expression using software from the BioRad 5000 Image system. (D) Expression of cyclin-D1 and cleaved PARP in individual tumors after treatment was determined by Western blot analysis using antibodies specific to cyclin-D1 and cleaved PARP, respectively. (E) A portion of FG cell-derived xenograft tumor samples was processed for histological examination. Analysis by H&E staining reveals cell death in different regions in tumors treated with Zt/g4-DM1, gemcitabine, or their combination but not in tumors from control mice. Arrows indicate dead regions and adjacent PDAC tissues in tumor masses.

alone had no effect on levels of RON expression. In addition, induction of cycle D1 expression was only observed in tumors treated with Zt/g4-DM1 or in combination with gemcitabine. Gemcitabine had no effect on cyclin-D1 expression, consistent with its mechanism of action [35]. Cleavage of PARP was observed in Zt/g4-DM1 and gemcitabine-treated tumors (**Figure 7D**). The PARP cleavage is a marker for cell apoptosis [36, 37]. Interestingly, an increase in the PARP cleavage was documented in the combination therapy, indicating a synergism between Zt/g4-DM1 and gemcitabine at molecular levels in enhancing PDAC cell apoptosis.

We further verified cell death in FG xenograft tumors collected from different groups (**Figure 7E**). Observation of H&E stained tumor slides found no morphological evidence of cell death from control mice (0/6, 0%). Gemcitabine treatment caused cell death at variable levels in tumor masses (6/6, 100%). Death regions in tumor masses also were observed in Zt/g4-DM1-treated mice (6/6, 100%). Similarly, the combination therapy resulted in massive tumor cell death (6/6, 100%). Since tumor samples were processed randomly, we were unable to quantitatively determine the severity of cell death that occurred in individual samples. Nonetheless, we confirmed that Zt/g4-DM1 alone or in combination with gemcitabine causes PDAC cell death in tumor masses.

Discussion

This report validates the preclinical efficacy of anti-RON ADC Zt/g4-DM1 for potential targeted therapy of PDAC. Zt/g4-DM1 treatment caused a rapid endocytosis of cell surface RON.

Internalized Zt/g4-DM1 resulted in cell cycle arrest in G2/M phase and reduction of cell viability followed by massive cell death. By analyzing the number of RON receptors expressed by PDAC cells, a correlation was established to predict the efficacy of Zt/g4-DM1 *in vitro* in killing PDAC cells. The PK study showed the dynamics of Zt/g4-DM1 in a two-compartment model with a terminal half-life of 6.05 days. PK parameters also projected the TSC of Zt/g4-DM1 at $\sim 3 \text{ mg/kg}$, which helped to model the time-dose relationship of Zt/g4-DM1 with its efficacy *in vivo*. Indeed, Zt/g4-DM1 at 20 mg/kg in the Q12 \times 2 regimen completely inhibited BxPC-3 xenograft tumor growth with a long-lasting effect up to 32 days. However, the correlation between the number of RON receptors and the level of inhibition *in vivo* was not established. Only partial inhibition was observed in FG and L3.6pl PDAC xenograft tumors. We further demonstrated that Zt/g4-DM1 in combination with gemcitabine shows the increase in tumor inhibition *in vitro*. Significantly, Zt/g4-DM1 in combination with gemcitabine was able to completely inhibit FG xenograft tumor growth *in vivo*. Thus, increased RON expression in PDAC cells is a suitable target for Zt/g4-DM1 directed PDAC therapy.

Increased expression in primary PDAC samples renders the RON receptor a suitable target for PDAC therapy using anti-Ron antibody-drug conjugate Zt/g4-DM1. Zt/g4-DM1 is a novel biotherapeutics with improved therapeutic index in our PDAC model. The binding of Zt/g4 results in a rapid and efficient internalization process with more than 80% of cell surface RON internalized within 48 h. In L3.6pl cells

expressing ~16,600 RON molecules per cell, it means the internalization of 13,300 RON receptors, equivalent to ~50,000 DM1 molecules entering into a single cell, which is sufficient to exert a biological activity. Flow cytometric analysis indicated that PDAC cell cycles arrest in G2/M phase, a feature of DM1 that impairs microtubule dynamics [38]. The effect was observed as early as 6 h after addition of Zt/g4-DM1 and characterized by progressive reduction of the G1 phase and the accumulation of cells at the G2/M phase. We also show the effectiveness of Zt/g4-DM1 in reduction of PDAC cell viability. We observed more than 80% reduction 96 h after Zt/g4-DM1 treatment. Moreover, we documented a massive cell death of PDAC cells in a Zt/g4-DM1 dose-dependent manner in three PDAC cell lines tested. Finally, we established an *in vitro* correlation between the number of RON molecules expressed by PDAC cells and the efficacy of Zt/g4-DM1, which demonstrates that PDAC cells expressing ~10,000 RON receptors on the cell surface are required for Zt/g4-DM1 to achieve the maximal cytotoxic effect. These observations suggest that Zt/g4-DM1-directed RON targeting is an effective strategy *in vitro* for killing PDAC cells.

Analysis of PK profiles provides insight into the dynamics of Zt/g4-DM1 *in vivo*. We found that the PK profile fits into the two-compartment model, similar to other clinically approved ADCs such as T-DM1 [39-41]. Also, we found no difference in the dynamics of Zt/g4-DM1 between tumor-bearing and -nonbearing mice, indicating that tumor growth does not alter the Zt/g4-DM1 PK profile [39]. Finally, we discovered that overexpression of RON by xenograft tumors plays no role in impacting the fate of Zt/g4-DM1 *in vivo*, suggesting that the PK of Zt/g4-DM1 is not affected by tissues/organs expressing RON. In other words, epithelial tissues constitutively expressing low levels of RON probably have very little impact on absorption, distribution, metabolism, and excretion of Zt/g4-DM1. Nonetheless, since our Zt/g4-DM1 does not recognize the mouse homologue of RON expressed by various tissues/organs, a PK profile of humanized Zt/g4-DM1 in human subjects should determine whether normal tissues/organs expressing low levels of RON affect the PK of Zt/g4-DM1 *in vivo*.

The obtained PK parameters help to determine the time-dose relationship of Zt/g4-DM1 in PDAC xenograft models, which projects the TSC *in vivo* and the dosing schedule for drug efficacy. In the BxPC-3 xenograft model highly sensitive to Zt/g4-DM1, we determined 3.02 mg/kg of Zt/g4-DM1 as the TSC according to the terminal half-life of Zt/g4-DM1 in conjunction with the tumor response curve (**Figure 4C**). The relationship also was validated in the model of CRC xenografts, in which Zt/g4-DM1 at 5 mg/kg was determined to be the TSC (**Figure 4B**). Subsequent studies using 20 mg/kg in the Q12 × 2 regimen confirmed the efficacy of Zt/g4-DM1 in inhibition of BxPC-3 xenograft tumor growth (**Figure 5A**). The TSC also determines the time intervals for administration of Zt/g4-DM1 at the Q12 for 20 mg/kg or the Q8 for 10 mg/kg regimen because the dose-schedule relationship determines the plasma drug concentrations over time and duration of time. The successful modeling of the time-dose schedule in the FG xenograft tumor model confirms the usefulness of PK parameters predicting outcomes (**Figures 5A and 7A**). However, the Zt/g4-DM1 responsiveness varied among three PDAC xenograft models. In the xenograft tumor model of L3.6pl cells, a highly malignant variant from COLO357 cell line [42], Zt/g4-DM1 at 20 mg/kg in the Q12 × 2 schedule initially inhibited L3.6pl xenograft tumor growth, but the efficacy decreased over time with accelerated tumor regrowth. In this sense, PK parameters for modeling the time-dose relationship of Zt/g4-DM1 have certain limitations. Nevertheless, the use of the time-dose relationship is suitable to determine the TSC for treatment of PDACs sensitive to Zt/g4-DM1.

The mechanism underlying the variable efficacies of Zt/g4-DM1 *in vivo* is currently unknown. Tumors initiated by L3.6pl cells expressing ~16,600 RON molecules are less sensitive than tumors formed by BxPC-3 cells with ~10,000 RON receptors. This indicates that the number of RON receptors is not well correlated *in vivo* with the efficacy of Zt/g4-DM1. Thus, the intrinsic natures of PDAC cells appear to be responsible for the sensitivity to Zt/g4-DM1. However, Zt/g4-DM1 is effective *in vivo* in elimination of RON-expressing PDAC cells as evident by the reduction of RON expression in Zt/g4-DM1-treated tumors (**Figure 5C, 5D**). The reduction was accompanied by

increased cyclin-D1 expression, PARP cleavage, and caspase-3 activation (**Figure 5E-G**), suggesting cell cycle changes in PDAC cells followed by activation of the apoptotic pathway. The consequence is the depletion of RON-expressing PDAC cells, resulting in accumulation of PDAC cells expressing no or low levels of RON. Thus, the selective enrichment of RON-negative cells constitutes the regrowth of xenograft tumors due to their insensitivity to Zt/g4-DM1. Accelerated regrowth of L3.6pl xenograft tumors after the second dose of Zt/g4-DM1 with minimal RON expression appears to support this notion.

The combination treatment showing complete inhibition of PDAC xenograft growth is an effective approach to enhance the Zt/g4-DM1 efficacy. *In vitro* Zt/g4-DM1 in combination with gemcitabine, oxaliplatin, and 5-FU displayed the synergistic effect in reduction of PDAC cell viability, indicating that the killing of PDAC cells can be synergized through different mechanisms of action. Studies *in vivo* of FG xenograft models further confirmed the synergism between Zt/g4-DM1 and gemcitabine on tumor growth. In the combination therapy, Zt/g4-DM1 and gemcitabine acted through different mechanisms to eliminate PDAC cells by regulating cell cycle and inducing apoptotic cell death. Thus, Zt/g4-DM1 in combination with chemotherapeutics could be a new strategy for targeted PDAC therapy in the future.

Acknowledgements

We thank Drs. AM Lowy for FG cells and GE Gallick for L3.6pl cells. We greatly appreciate Ms. Susan Denney (TTUHSC School of Pharmacy in Amarillo, TX) for editing the manuscript. This work was supported by NIH grant R01CA91980, funds from Amarillo Area Foundation, SKLDTID subproject #2011ZZ01 from SKLDTID at First Hospital of Zhejiang University School of Medicine, Hangzhou, China (MHW) and by Zhejiang Major Medical Health & Science Technology Foundation Projects #WKJ-ZJ-13 and #2014C33204 (HPY). *: LF and HPY contributed equally to this work.

Disclosure of conflict of interest

None.

Address correspondence to: Dr. Ming-Hai Wang, Department of Biomedical Sciences, TTUHSC Sch-

ool of Pharmacy, 1406 Coulter Street, Amarillo, TX 79106, USA. Tel: 806-414-9214; Fax: 806-356-4770; E-mail: minghai.wang@ttuhsc.edu

References

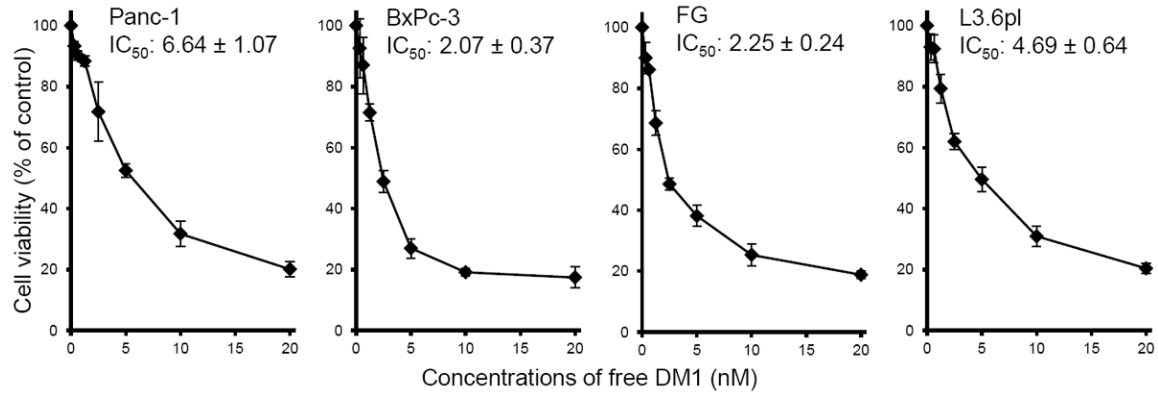
- [1] Ryan DP, Hong TS and Bardeesy N. Pancreatic adenocarcinoma. *N Engl J Med* 2014; 371:1039-1049.
- [2] Vaccaro V, Gelibter A, Bria E, Iapicca P, Cappello P, Di Modugno F, Pino MS, Nuzzo C, Cognetti F, Novelli F, Nistico P and Milella M. Molecular and genetic bases of pancreatic cancer. *Curr Drug Targets* 2012; 13: 731-743.
- [3] Morris JP 4th, Wang SC and Hebrok M. KRAS, Hedgehog, Wnt and the twisted developmental biology of pancreatic ductal adenocarcinoma. *Nat Rev Cancer* 2010; 10: 683-695.
- [4] Bardeesy N and DePinho RA. Pancreatic cancer biology and genetics. *Nat Rev Cancer* 2002; 2: 897-909.
- [5] Jamieson NB, Carter CR, McKay CJ and Oien KA. Tissue biomarkers for prognosis in pancreatic ductal adenocarcinoma: a systematic review and meta-analysis. *Clin Cancer Res* 2011; 17: 3316-3331.
- [6] Fong ZV and Winter JM. Biomarkers in pancreatic cancer: diagnostic, prognostic, and predictive. *Cancer J* 2012; 18: 530-538.
- [7] Ronsin C, Muscatelli F, Mattei MG and Breathnach R. A novel putative receptor protein tyrosine kinase of the met family. *Oncogene* 1993; 8: 1195-1202.
- [8] Yao HP, Zhou YQ, Zhang R and Wang MH. MSP-RON signaling in cancer: pathogenesis and therapeutic potential. *Nat Rev Cancer* 2013; 13: 466-481.
- [9] Tamagnone L and Comoglio PM. Control of invasive growth by hepatocyte growth factor (HGF) and related scatter factors. *Cytokine Growth Factor Rev* 1997; 8: 129-142.
- [10] Camp ER, Yang A, Gray MJ, Fan F, Hamilton SR, Evans DB, Hooper AT, Pereira DS, Hicklin DJ and Ellis LM. Tyrosine kinase receptor RON in human pancreatic cancer: expression, function, and validation as a target. *Cancer* 2007; 109: 1030-1039.
- [11] Thomas RM, Toney K, Fenoglio-Preiser C, Revelo-Penafiel MP, Hingorani SR, Tuveson DA, Waltz SE and Lowy AM. The RON receptor tyrosine kinase mediates oncogenic phenotypes in pancreatic cancer cells and is increasingly expressed during pancreatic cancer progression. *Cancer Res* 2007; 67: 6075-6082.
- [12] Logan-Collins J, Thomas RM, Yu P, Jaquish D, Mose E, French R, Stuart W, McClaine R, Aronow B, Hoffman RM, Waltz SE and Lowy AM. Silencing of RON receptor signaling promotes apoptosis and gemcitabine sensitivity in pancreatic cancers. *Cancer Res* 2010; 70: 1130-1140.

- [13] Jaquish DV, Yu PT, Shields DJ, French RP, Maruyama KP, Niessen S, Hoover H, A Cheresch D, Cravatt B and Lowy AM. IGF1-R signals through the RON receptor to mediate pancreatic cancer cell migration. *Carcinogenesis* 2011; 32: 1151-1156.
- [14] Padhye SS, Guin S, Yao HP, Zhou YQ, Zhang R and Wang MH. Sustained expression of the RON receptor tyrosine kinase by pancreatic cancer stem cells as a potential targeting moiety for antibody-directed chemotherapeutics. *Mol Pharm* 2011; 8: 2310-2319.
- [15] Yu PT, Babicky M, Jaquish D, French R, Marayuma K, Mose E, Niessen S, Hoover H, Shields D, Cheresch D, Cravatt BF and Lowy AM. The RON-receptor regulates pancreatic cancer cell migration through phosphorylation-dependent breakdown of the hemidesmosome. *Int J Cancer* 2012; 131: 1744-1754.
- [16] Tactacan CM, Chang DK, Cowley MJ, Humphrey ES, Wu J, Gill AJ, Chou A, Nones K, Grimmond SM, Sutherland RL, Biankin AV and Daly RJ; Australian Pancreatic Genome Initiative. RON is not a prognostic marker for resectable pancreatic cancer. *BMC Cancer* 2012; 12: 395-403.
- [17] Zeng JY, Sharma S, Zhou YQ, Yao HP, Hu X, Zhang R and Wang MH. Synergistic activities of MET/RON inhibitor BMS-777607 and mTOR inhibitor AZD8055 to polyploid cells derived from pancreatic cancer and cancer stem cells. *Mol Cancer Ther* 2014; 13: 37-48.
- [18] Wang MH, Lee W, Luo YL, Weis MT and Yao HP. Altered expression of the RON receptor tyrosine kinase in various epithelial cancers and its contribution to tumorigenic phenotypes in thyroid cancer cells. *J Pathol* 2007; 213: 402-411.
- [19] O'Toole JM, Rabenau KE, Burns K, Lu D, Mangalampalli V, Balderes P, Covino N, Bassi R, Prewett M, Gottfredsen KJ, Thobe MN, Cheng Y, Li Y, Hicklin DJ, Zhu Z, Waltz SE, Hayman MJ, Ludwig DL and Pereira DS. Therapeutic implications of a human neutralizing antibody to the macrophage-stimulating protein receptor tyrosine kinase (RON), a c-MET family member. *Cancer Res* 2006; 66: 9162-9170.
- [20] Zou Y, Howell GM, Humphrey LE, Wang J and Brattain MG. Ron knockdown and Ron monoclonal antibody IMC-RON8 sensitize pancreatic cancer to histone deacetylase inhibitors (HDACi). *PLoS One* 2013; 8: e69992.
- [21] Yao HP, Zhou YQ, Ma Q, Guin S, Padhye SS, Zhang RW and Wang MH. The monoclonal antibody Zt/f2 targeting RON receptor tyrosine kinase as potential therapeutics against tumor growth-mediated by colon cancer cells. *Mol Cancer* 2011; 10: 82-92.
- [22] Guin S, Yao HP and Wang MH. RON receptor tyrosine kinase as a target for delivery of chemodrugs by antibody directed pathway for cancer cell cytotoxicity. *Mol Pharm* 2010; 7: 386-397.
- [23] Kawada I, Hasina R, Arif Q, Mueller J, Smithberger E, Husain AN, Vokes EE and Salgia R. Dramatic antitumor effects of the dual MET/RON small-molecule inhibitor LY-2801653 in non-small cell lung cancer. *Cancer Res* 2014; 74: 884-895.
- [24] Schroeder GM, An Y, Cai ZW, Chen XT, Clark C, Cornelius LA, Dai J, Gullo-Brown J, Gupta A, Henley B, Hunt JT, Jeyaseelan R, Kamath A, Kim K, Lippy J, Lombardo LJ, Manne V, Oppenheimer S, Sack JS, Schmidt RJ, Shen G, Stefanski K, Tokarski JS, Trainor GL, Wautlet BS, Wei D, Williams DK, Zhang Y, Zhang Y, Fargnoli J and Borzilleri RM. Discovery of N-(4-(2-amino-3-chloropyridin-4-yloxy)-3-fluorophenyl)-4-ethoxy-1-(4-fluorophenyl)-2-oxo-1,2-dihydropyridine-3-carboxamide (BMS-777607), a selective and orally efficacious inhibitor of the Met kinase superfamily. *J Med Chem* 2009; 52: 1251-1254.
- [25] Zhang Y, Kaplan-Lefko PJ, Rex K, Yang Y, Moriguchi J, Osgood T, Mattson B, Coxon A, Reese M, Kim TS, Lin J, Chen A, Burgess TL and Dussault I. Identification of a novel receptor d'origine nantais/c-met small-molecule kinase inhibitor with antitumor activity in vivo. *Cancer Res* 2008; 68: 6680-6687.
- [26] Feng L, Yao HP, Wang W, Zhou YQ, Zhou J, Zhang R and Wang MH. Efficacy of Anti-RON Antibody Zt/g4-Drug Maytansinoid Conjugation (Anti-RON ADC) as a Novel Therapeutics for Targeted Colorectal Cancer Therapy. *Clin Cancer Res* 2014; 20: 1-14.
- [27] Sievers EL and Senter PD. Antibody-drug conjugates in cancer therapy. *Annu Rev Med* 2013; 64: 15-29.
- [28] Teicher BA. Antibody drug conjugates. *Curr Opin Oncol* 2014; 26: 476-483.
- [29] Scott AM, Wolchok JD, Old LJ. Antibody therapy of cancer. *Nat Rev Cancer* 2012; 12: 278-287.
- [30] Ensinger C and Sterlacci W. Implications of EGFR PharmDx kit for cetuximab eligibility. *Expert Rev Mol Diagn* 2008; 8: 141-148.
- [31] Musgrove EA, Caldon CE, Barraclough J, Stone A and Sutherland RL. Cyclin D as a therapeutic target in cancer. *Nat Rev Cancer* 2011; 11: 558-572.
- [32] Yao HP, Luo YL, Feng L, Cheng LF, Lu Y, Li W and Wang MH. Agonistic monoclonal antibodies potentiate tumorigenic and invasive activities of splicing variant of the RON receptor tyrosine kinase. *Cancer Biol Ther* 2006; 5: 1179-1186.

Anti-RON ADC for pancreatic cancer therapy

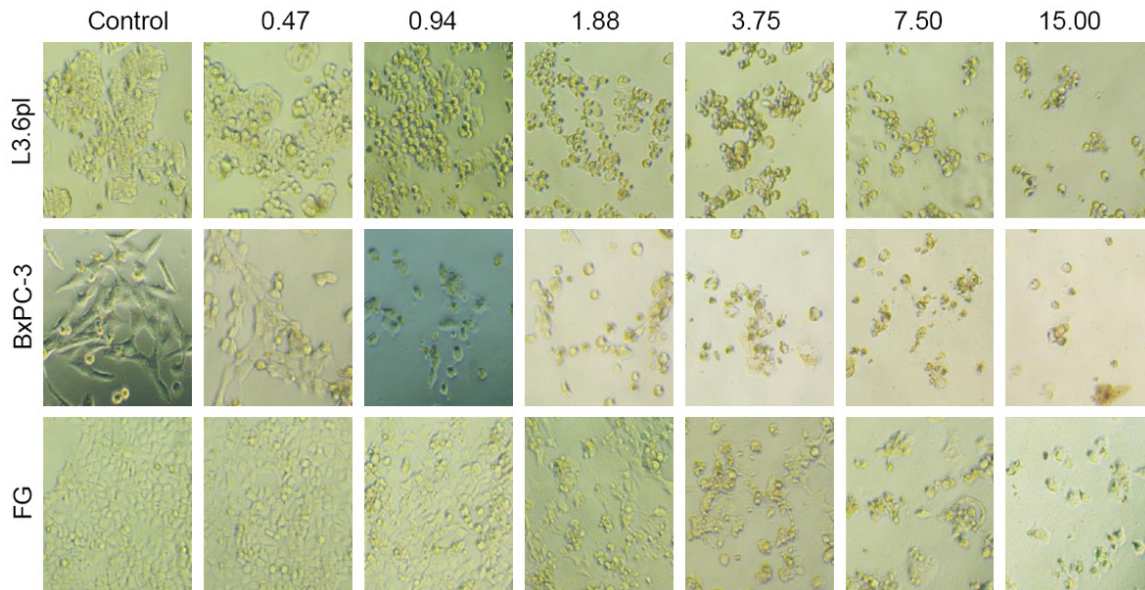
- [33] Chou TC. Theoretical basis, experimental design, and computerized simulation of synergism and antagonism in drug combination studies. *Pharmacol Rev* 2006; 58: 621-681.
- [34] Chou TC. Drug combination studies and their synergy quantification using the Chou-Talalay method. *Cancer Res* 2010; 70: 440-446.
- [35] Plunkett W, Huang P, Xu YZ, Heinemann V, Grunewald R and Gandhi V. Gemcitabine: metabolism, mechanisms of action, and self-potentiation. *Semin Oncol* 1995; 22 Suppl 11: 3-10.
- [36] Luo X and Kraus WL. On PAR with PARP: Cellular stress signaling through poly(ADP-ribose) and PARP-1. *Genes Dev* 2012; 26: 417-432
- [37] Duriez PJ and Shah GM. Cleavage of poly(ADP-ribose) polymerase: a sensitive parameters to study cell death. *Biochem Cell Biol* 1997; 75: 337-349.
- [38] Lopus M, Oroudjev E, Wilson L, Wilhelm S, Widdison W, Chari R and Jordan MA. Maytansine and cellular metabolites of antibody-maytansinoid conjugates strongly suppress microtubule dynamics by binding to microtubules. *Mol Cancer Ther* 2010; 9: 2689-2699.
- [39] Jumbe NL, Xin Y, Leipold DD, Crocker L, Dugger D, Mai E, Sliwkowski MX, Fielder PJ and Tibbitts J. Modeling the efficacy of trastuzumab-DM1, an antibody drug conjugate, in mice. *J Pharmacokinet Pharmacodyn* 2010; 37: 221-242.
- [40] Sapra P, Betts A and Boni J. Preclinical and clinical pharmacokinetic/pharmacodynamic considerations for antibody-drug conjugates. *Expert Rev Clin Pharmacol* 2013; 6: 541-555.
- [41] Wang J, Song P, Schrieber S, Liu Q, Xu Q, Blumenthal G, Amiri Kordestani L, Cortazar P, Ibrahim A, Justice R, Wang Y, Tang S, Booth B, Mehrotra N and Rahman A. Exposure-response relationship of T-DM1: insight into dose optimization for patients with HER2-positive metastatic breast cancer. *Clin Pharmacol Ther* 2014; 95: 558-564.
- [42] Bruns CJ, Harbison MT, Kuniyasu H, Eue I and Fidler IJ. In vivo selection and characterization of metastatic variants from human pancreatic adenocarcinoma by using orthotopic implantation in nude mice. *Neoplasia* 1999; 1: 50-62.

Anti-ROn ADC for pancreatic cancer therapy



Supplementary Figure 1. Effect of free DM1 *in vitro* on cell viability of PDAC cell lines. Four PDAC cell lines (8000 cells per well in a 96-well plate in triplicate) were treated with different amounts of DM1 for 96 h. Cells without treatment were used as the control. Cell viability was determined by the MTS assay. Individual IC₅₀ values for each cell line were calculated using GraphPad Prism 6 software. Results shown here were from one of three experiments with similar results.

Zt/g4-DM1 (µg/ml):



Supplementary Figure 2. Death of PDAC cells after Zt/g4-DM1 treatment: Three PDAC cell lines were cultured at 8000 cells per well in a 96-well culture plate in triplicate and treated with different amount of Zt/g4-DM1 for 96 h. Morphological changes were observed under the Olympus BK-41 inverted microscope and photographed. Images showing cell death are presented. Quantitative analysis of cell death was presented in **Figure 3E**. One of two experiments with similar results.